NONLINEAR SCATTERING EFFECTS IN OPTICAL FIBERS

S. P. Singh [†]**, R. Gangwar, and N. Singh**

Department of Electronics and Communication
University of Allahabad
Allahabad-211002, India

Abstract—The nonlinear scattering effects in optical fiber occur due to inelastic-scattering of a photon to a lower energy photon. This paper describes stimulated Brillouin scattering and stimulated Raman scattering processes. Their thresholds, reduction in power penalty and applications along with comparative study of these effects are also presented.

1. INTRODUCTION

The nonlinear scattering effects in optical fibers are due to the inelastic scattering of a photon to a lower energy photon. The energy difference is absorbed by the molecular vibrations or phonons in the medium. In other words one can state that the energy of a light wave is transferred to another wave, which is at a higher wavelength (lower energy) such that energy difference appears in form of phonons [1]. The other wave is known as the Stokes wave. The signal can be considered as pump wave. Of course, high-energy photon at the so-called anti-Stokes frequency can also be created if phonon of right energy and momentum is available.

There are two nonlinear scattering phenomenon in fibers and both are related to vibrational excitation modes of silica [2–6, 31–33]. These phenomenon are known as stimulated Raman scattering (SRS) and stimulated Brillouin scattering (SBS). The fundamental difference is that, the optical phonons participate in SRS while SBS is through acoustic phonons. As a result of this difference, SBS occurs only in one direction i.e., backward while SRS can occur in both directions-forward and backward.

[†] Also with Physics Department, KNIPSS, Sultanpur (U. P.), India.

The nonlinear scattering processes cause disproportionate attenuation at high optical power levels. It also causes the transfer of optical power from one mode to other modes in forward or backward direction at different frequency. In fact the stimulated scattering mechanisms (SBS or SRS) also provide optical gain but with a shift in frequency. This paper is organized as follows:

Stimulated Brillouin scattering is discussed in Section 2. Its threshold, reduction in power penalty and applications are presented in subsections. The stimulated Raman scattering is given in Section 3. The threshold, reduction in power penalty and applications of SRS process are presented in subsections of this section. Both processes are compared under Section 4, and Section 5 presents comparison of scattering effects with Kerr effect. Finally, conclusion is given in Section 6.

2. STIMULATED BRILLOUIN SCATTERING (SBS)

Classically, the thermally generated density fluctuations of a material medium are responsible for scattering of light. These density fluctuations result in compression and rarefaction regions within the medium, and may be considered as consist of two components, the propagating component and the non-propagating component. When a light wave is incident, scattering from the non-propagating component gives the central Rayleigh line and scattering from the propagating component results in Brillouin lines. There is finite width in Brillouin and Rayleigh lines. The propagating component of density fluctuations behaves as a sound wave of high frequency. The damping of such a wave in the material medium is responsible for finite width in Brillouin lines while non-zero lifetime of the non-propagating component produces width in Rayleigh lines.

2.1. Basic Theory

Brillouin scattering is a nonlinear process that can occur in optical fibers at large intensity. The large intensity produces compression (due to electric field also known as pump field) in core of fiber through the process known as electrostriction [1]. This phenomenon produces density-fluctuations in fiber medium. It increases the material disorder, which in turn modulates the linear refractive index of medium and results in an electrostrictive-nonlinearity [4]. The modulated refractive index behaves as an index grating, which is pump-induced. The scattering of pump light through Bragg diffraction by the pump-induced index grating is called as Brillouin scattering. The disorder

is time dependent so the scattered light is shifted (Brillouin shift) in frequency by the frequency of sound wave. For pulses shorter than 500 ps, there is no spatial overlap between the pulse and acoustic wave, which results in negligible electrostrictive nonlinearity [5].

Quantum mechanically the Brillouin shift originates from the photon-phonon interaction, and associated Doppler displacement. In this interaction either a phonon is annihilated (Stokes process-positive Brillouin shift) or created (anti-stokes process-negative Brillouin shift).

2.2. Physical Process

For an oscillating electric field at the pump frequency ω_P, the electrostriction process generates a macroscopic acoustic wave (involved phonons are coherent) at some frequency ω_B. The Brillouin scattering may be spontaneous or stimulated (Figure 1(a) and 1(b)). In spontaneous Brillouin scattering, there is annihilation of a pump photon, which results in creation of Stokes photon and an acoustic phonon simultaneously. The conservation laws for energy and momentum must be followed in such scattering processes.

For energy conservation, the Stokes shift ω_B must be equal to $(\omega_P - \omega_S)$, where ω_P and ω_S are frequencies of pump and Stokes waves. The momentum conservation requires $\boldsymbol{k}_A = (\boldsymbol{k}_P - \boldsymbol{k}_S)$, where $\boldsymbol{k}_A$, $\boldsymbol{k}_P$ and $\boldsymbol{k}_S$ are momentum vectors of acoustic, pump and Stokes waves respectively.

If v_A is acoustic velocity then dispersion relation [6] can be written as

$$\omega_B = v_A \left| \overrightarrow{k_A} \right| = v_A \left| \overrightarrow{k_P} - \overrightarrow{k_S} \right|$$

$$\text{or} \qquad \omega_B = 2v_A \left| \overrightarrow{k_P} \right| \sin\frac{\theta}{2} \tag{1}$$

where θ is the angle between the pump and Stokes momentum vectors and modulas of $\boldsymbol{k}_P$ and $\boldsymbol{k}_S$ is taken as nearly equal. From above expression, it is clear that the frequency shift depends on angle θ. For $\theta = 0°$, shift is zero i.e., there is no frequency shift in forward direction (no Brillouin scattering). The $\theta = \pi$ represents backward direction and in this situation the shift is maximum. The maximum backward frequency shift ($\nu_B = \omega_B/2\pi$) is calculated from Equation (1) and the relationship $\left| \overrightarrow{k_P} \right| = 2\pi n/\lambda_P$ as

$$\nu_B = \frac{2nv_A}{\lambda_P} \tag{2}$$
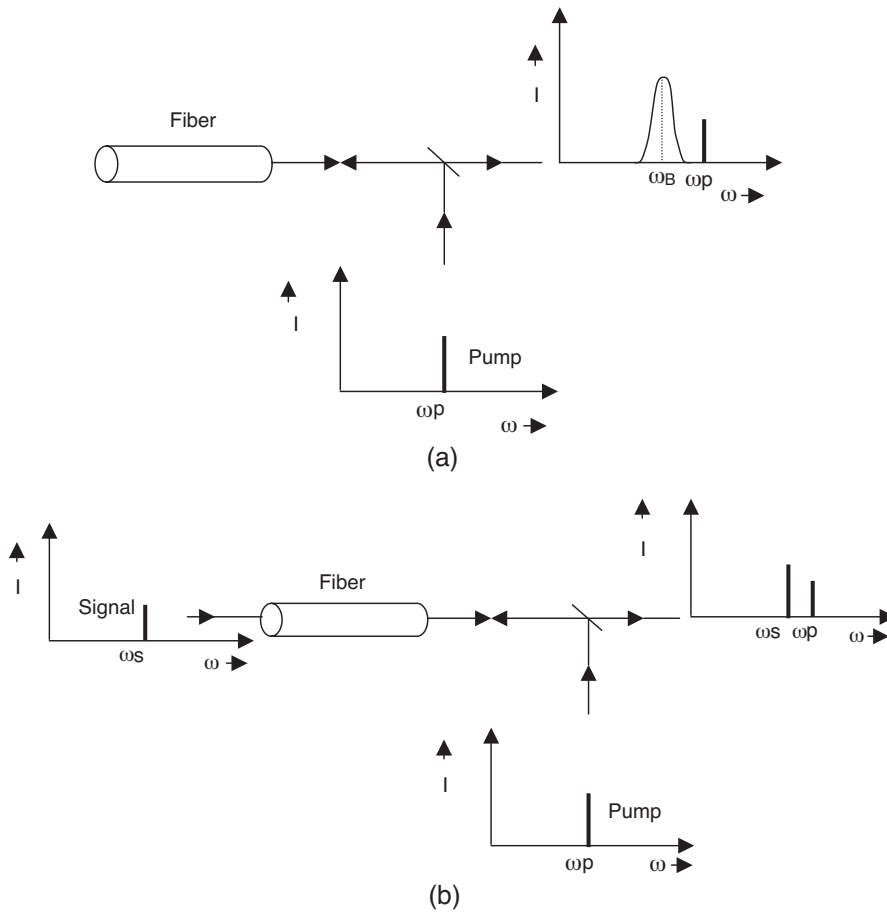
where n is the mode index.

Figure 1. (a) Spontaneous Brillouin scattering phenomenon. (b) Stimulated Brillouin scattering phenomenon.

In single mode fibers, the spontaneous Brillouin scattering may occur in forward direction also. The reason behind this is that there is relaxation of the wave vector selection rule due to guided nature of acoustic waves. This process is known as guided acoustic wave Brillouin scattering [6]. In this case a small amount of extremely weak light is generated.

When scattered wave is produced spontaneously, it interferes with the pump beam. This interference generates spatial modulation in intensity, which results in amplification of acoustic wave by the electrostriction effect (elasto-optic effect). The amplified acoustic

wave in turn raises the spatial modulation of intensity and hence the amplitude of scattered wave. Again there is increment in amplitude of acoustic wave. This positive feedback dynamics is responsible for the stimulated Brillouin scattering, which ultimately, can transfer all power from the pump to the scattered wave.

2.3. Brillouin Gain Spectrum

From the Brillouin gain spectrum, the dependence of gain on frequency can be described. The finite life time T_B of acoustic phonons (the damping time of acoustic wave responsible for Brillouin scattering) is root cause of frequency dependence of the gain (g_B) [7, 8]. This is also a reason for small spectral width of the gain spectrum. The nature of decay of acoustic waves is exponential like $\exp[-t/T_B]$. The Brillouin gain [9] may be written as

$$g_B(\omega) = \frac{g_B(\omega_B)}{1 + (\omega - \omega_B)^2 \, T_B^2} \tag{3}$$

The peak value of Brillouin gain occurs at $\omega = \omega_B$. The gain $g_B(\omega)$ depends on many parameters like concentration of dopants in fiber, inhomogeneous distribution of dopants and the electrostrictive coefficient. Figure 2 describes the Brillouin gain spectra at pump wavelength 1525 nm for (a) silica-core fiber, (b) depress-cladding fiber and (c) dispersion shifted fiber (c).
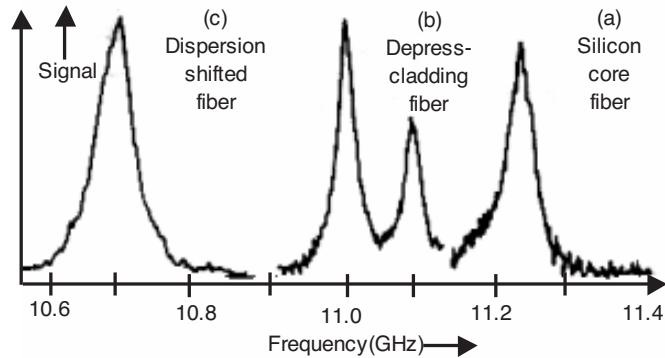

Figure 2. Brillouin-gain spectra at pump wavelength 1525 nm.

It may be observed from Figure 2 that the Brillouin shift [10] in case of fibers (b) and (c) is small as compared to fiber (a). The reason is the higher germania concentration in the fiber core of fibers (b) and

(c). The inhomogeneous distribution of germania within the core of fiber (b) is responsible for double peak in Brillouin gain spectrum of fiber (b).
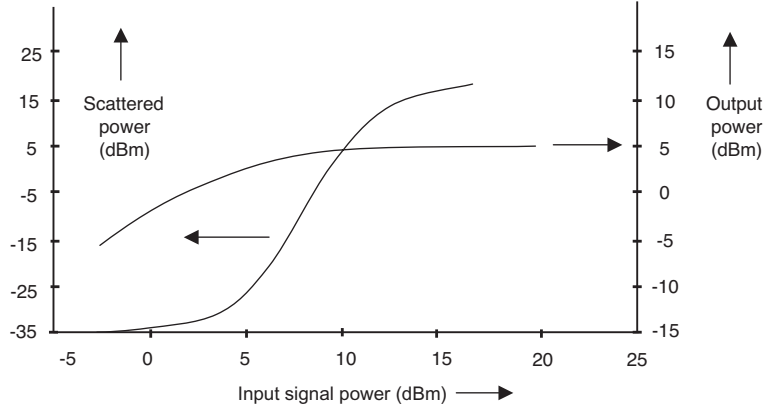

Figure 3. Effect of SBS on signal power for 13 km DSF.

2.4. Threshold Power

Taking into consideration the interaction between pump and Stokes wave, the initial growth of Stokes wave under CW and quasi-CW condition, can be written as

$$\frac{dI_S}{dz} = g_B I_P I_S \tag{4}$$

where g_B is Brillouin gain coefficient, I_P and I_S are the pump and Stokes wave intensities respectively.

The Brillouin scattering produces photons within the bandwidth of Brillouin-gain spectrum and hence all frequency components will be amplified. The frequency component for which g_B is maximum, builds up rapidly and nature will be almost exponential. For pure silica, g_B is maximum for frequency component which is downshifted from pump frequency by about 11 GHz.

Keeping in mind the fiber losses at Stokes frequency and counterpropagating nature of Stokes wave, the Equation (4) can be written as [6]

$$\frac{dI_S}{dz} = -g_B I_P I_S + \alpha_S I_S \tag{5}$$

For pump wave the coupled equation can be given as

$$\frac{dI_P}{dz} = -\frac{\omega_P}{\omega_S} g_B I_P I_S - \alpha_P I_P \tag{6}$$

where α_P is responsible for fiber losses at pump frequency.

The feedback process responsible for Brillouin scattering [1] is controlled by two coupled equations, (5) and (6). For simplicity one may consider $\omega_P \approx \omega_S$ and therefore $\alpha_P \approx \alpha_S \equiv \alpha$ (due to small Brillouin shift). Now the coupled equations can be written as

$$\frac{dI_S}{dz} = -g_B I_P I_S + \alpha I_S \tag{7}$$

and

$$\frac{dI_P}{dz} = -g_B I_P I_S - \alpha I_P \tag{8}$$

In absence of fiber losses $\alpha = 0$, Equations (7) and (8) can be reduced to,

$$(I_S - I_P) = \text{constant} \tag{9}$$

This expression describes the conservation phenomenon on light energy during the Brillouin process.

The threshold power is a minimum power level at which the effect of nonlinearity starts. It is incident power at which the pump and Stokes powers are equal at the fiber output.

In case where the Stokes power is much smaller than the pump power, one can assume that pump power is not depleted and therefore the term $-g_B I_P I_S$ in Equation (8) can be neglected.

$$\frac{dI_P}{dz} = -\alpha I_P \tag{10}$$

The solution of above equation can be obtained as

$$I_P(z) = I_P(0) \exp[-\alpha z] \tag{11}$$

where $I_P(z)$ and $I_P(0)$ are pump intensities at length z and at $z = 0$ respectively.

Now from Equations (7) and (11), we have

$$\frac{dI_S}{dz} = -g_B I_P(0) \exp[-\alpha z] I_S + \alpha I_S \tag{12}$$

Solution of this equation can be written as,

$$I_S(0) = I_S(L) \exp[g_B I_P(0) L_{eff} - \alpha L] \tag{13}$$

where L_{eff} is effective length of interaction. It is slightly less than fiber length L because of pump absorption.

Equation (13) and Equation (11) can be written as

$$P_S(0) = P_S(L) \exp(-\alpha L) \exp\left(\frac{g_B P_P(0) L_{eff}}{A_{eff}}\right) \qquad (14)$$

and

$$P_P(L) = P_P(0) \exp[-\alpha L] \qquad (15)$$

where intensities are related to power as $P_S = A_{eff} I_S$ and $P_P = A_{eff} I_P$. The A_{eff} is the effective core area of the fiber.

The threshold power can be calculated from Equation (14) and Equation (15). It can be approximated as [11]

$$P_{th} \approx \frac{21 b A_{eff}}{g_B L_{eff}} \qquad (16)$$

Here the value of polarization factor b lies between 1 and 2 depending on relative polarization of pump and Stokes waves [12]. Typically $A_{eff} \approx 50\,\mu m^2$, $L_{eff} \approx 20\,km$ and $g_B = 4 \times 10^{-11}\,m/W$ for an optical system at 1550 nm. With these values and taking $b = 1$, $P_{th} \approx 1.3\,mW$. Because of such a low value of threshold level, the SBS process is a dominant nonlinear process in fibers.

The threshold power becomes just double if polarization factor b is taken equal to 2. The threshold power (P_{th}) depends mainly on the Brillouin gain (g_B). The fiber in homogeneousness affects g_B and hence P_{th} .The variation in dopant also affects SBS threshold power upto some extent.

When threshold is reached the effect of SBS on the signal power [13] is described by the Figure 3. The Brillouin-scattered power and signal power transmitted is plotted as a function of signal input power. Upto the threshold power, the transmitted power increases linearly. When scattered power attains the value equal to threshold power, the transmitted power becomes constant and independent of input signal power.

2.5. Reduction in Power Penalty

When any nonlinear effect contributes to signal impairment, an additional amount of power is needed at the receiver to maintain the same BER as in absence of nonlinear effects.

There are many ways to reduce the power penalty due to SBS [14–16].

1. Keep the power level per WDM channel much below the SBS threshold. In long-haul systems one may have to reduce the amplifier spacing.

2. The effect of small gain bandwidth of SBS phenomenon can be decreased by increasing the linewidth of the source used. The linewidth can be increased because of chirping effect by direct modulation of source laser. This may results in significant dispersion penalty, which can be reduced by suitable dispersion management.

3. Phase modulation methods in place of amplitude modulation methods reduce the power present in optical fiber, which in turn reduces the SBS penalty.

2.6. Applications of SBS Phenomenon

Normally SBS puts limitations on optical communication systems, but with suitable system arrangement it can be useful for making many optical devices. These are described below.

Fiber Sensors

The fiber sensors are capable of sensing the temperature and strain over long distances [17, 18]. Whenever there is change in temperature or strain, the refractive index of silica changes in response to such variations. This change produces change in Brillouin shift. By registering the change in Brillouin shift the distribution of temperature and strain over long distances can be obtained. Sometimes such sensors are also known as distributed fiber sensors.

Several methods have been introduced to improve sensing performance in four key areas: spatial resolution, measurement accuracy, total sensing length and measurement-acquisition time. These factors are generally interrelated and improvement in one factor may results in degradation in one or more of the others. Dark-pulse Brillouin optical time domain analysis (BOTDA) technique [34] provides improved resolution, accuracy and acquisition time over conventional BOTDA systems without the severe limitations on sensing length often imposed by other high-resolution techniques.

Brillouin Fiber Amplifiers

The optical gain in SBS process can be utilized in amplification of weak signal provided the frequency shift of weak signal from pump frequency is equal to Brillouin shift. In Brillouin fiber amplifier (Figure 4), a part of pump power is transmitted to signal through the SBS process and hence amplification in signal power occurs [19].

When power level inside silica fiber exceeds the threshold level (P_{th}), the stimulated Brillouin scattering starts due to a positive feedback dynamics set up inside the fiber medium. This dynamics results in amplification of the signal. The Brillouin fiber amplifiers
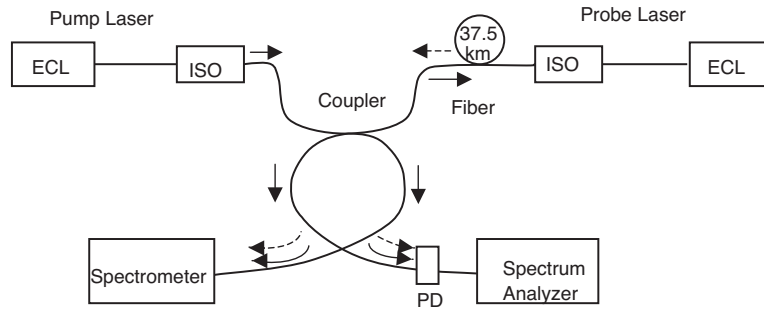
Figure 4. Schematic illustration of a Brillouin amplifier. Solid and dashed arrows show path of pump and probe lasers. ECL-External cavity laser, ISO-Isolater, and PD-Photodetector.

are less suitable as power amplifier, preamplifier or in-line amplifier in lightwave systems due to their narrow bandwidth [8]. But this characteristic is advantageous in coherent and multichannel communication systems. It is this feature, which is exploited in selective amplification and in tunable narrow band optical filter for channel selection.

Brillouin amplification can be exploited in generation of slow light in a short length of highly nonlinear bismuth-oxide fiber. A five-fold reduction in group velocity for about 200 ns pulse can be obtained by using 2 m of fiber [35].

Beam Combiner

Stimulated Brillouin scattering (SBS) can be exploited in passive combination of multiple beams in a fiber [36]. Four off-axis beams are combined in a long multimode optical fiber using a novel all-optical mount. The beam that comes out has spatial coherence properties of LP_{01} mode. By using off-axis pumps, the threshold of SBS can be raised several times in comparison to on-axis pump beams. This method may be helpful in increasing the brightness of array of fiber amplifiers.

Pulse Delaying and Advancement

The stimulated Brillouin scattering process is helpful in controlling the group velocity of an optical pulse as it travels along fiber [37, 38]. The changes in group index of 10-3 in several kilometer length of fiber have been achieved experimentally. This leads to pulse delaying and advancement in the range of tens of nanoseconds. These group delay changes can be obtained in conventionally used optical fibers.

Pipeline Buckling Detection

For the pipe with internal pressure, concentric load, and bending load, a localized pipe-wall buckling takes place away from the middle of the pipe. A distributed Brillouin fiber sensor can be used to detect localized pipe-wall buckling in an energy pipe [39]. This can be achieved by measuring the longitudinal and hoop strain distributions. The locations of such buckling are found and distinguished using strain-load data.
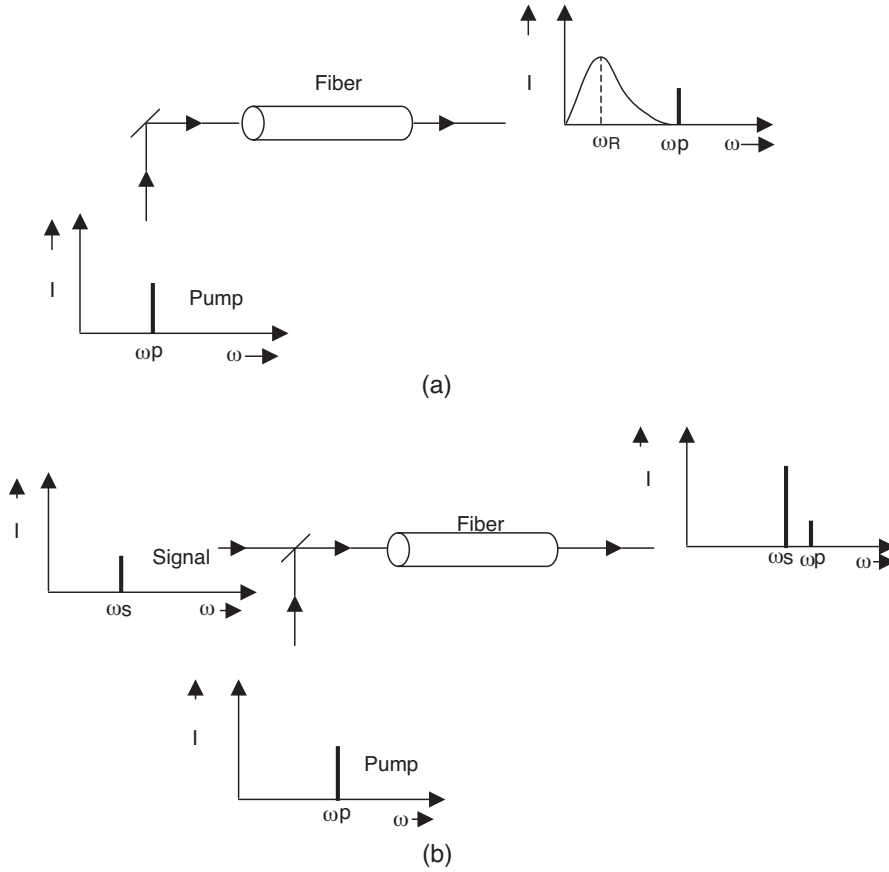

Figure 5. (a) Spontaneous Raman scattering phenomenon. (b) Stimulated Raman scattering phenomenon.

3. STIMULATED RAMAN SCATTERING

The Raman scattering effect is the inelastic scattering [1] of a photon with an optical phonon, which originates from a finite response time of the third order nonlinear polarization [20] of the material. When a monochromatic light beam propagates in an optical fiber, spontaneous Raman scattering (Figure 5(a)) occurs. It transfers some of the photons to new frequencies. The scattered photons may lose energy (Stokes shift) or gain energy (anti-Stokes shift). If the pump beam is linearly polarized, the polarization of scattered photon may be the same (parallel scattering) or orthogonal (perpendicular scattering). If photons at other frequencies are already present then the probability of scattering to those frequencies is enhanced. This process is known as stimulated Raman scattering (Figure 5(b)).

In stimulated Raman scattering, a coincident photon at the downshifted frequency will receive a gain. This feature of Raman scattering is exploited in Raman amplifiers for signal amplification.

3.1. Basic Theory

Raman scattering is a weak effect in comparison to Rayleigh scattering. It occurs due to slight modulation of the refractive index through molecular vibration of material [2, 15]. A photon with energy $\hbar\omega_P$ traveling through a material can excite a vibrational transition of the material forming optical phonon with energy $\hbar\omega_V$ and a photon with slightly reduced energy $\hbar\omega_S$ (Figure 6) such that:

$$\hbar\omega_S = \hbar\omega_P - \hbar\omega_V$$

The modulation in refractive index is taken into account through discussion of polarizability of material in case of Raman scattering process. To understand this, the classical model of Raman scattering may be a simple way. In this model, it is assumed that electrons are attached to an atom through a spring, and the strength of the spring is assumed to depend on the position of the atom. If atom is in vibrational motion with angular frequency ω_V, then spring constant is modulated at angular frequency ω_P. If a light wave of angular frequency ω_P propagates through the material, the motion of electron will be amplitude modulated sinusoidal motion. Therefore the radiation generated by the electron will also be amplitude modulated. This radiation has components $\omega_P \pm \omega_V$ corresponding to Stokes and anti-Stokes Raman scattering.

When a light wave with angular frequency ω is incident on the material, the electric field vector will induce a dipole moment p such
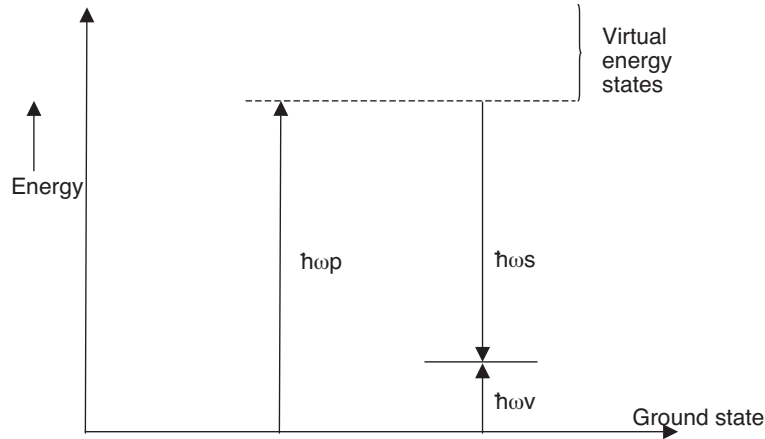
Figure 6. Schematic representation of Raman scattering.

that:
$$p = \alpha E \tag{17}$$

where α is molecular polrizability and E is electric field vector. The α measures the resistance of the particle to the displacement of its electron cloud.

For harmonic electric field $E(t) = E_0 \exp(j\omega_P t)$, the variation of α with time can be written as

$$\alpha(t) = \alpha_0 + \left(\frac{\partial \alpha}{\partial x}\right)_{x_0} dx(t) \tag{18}$$

Here $dx(t)$ is the displacement from the equilibrium molecular length x_0 such that

$$dx(t) = dx_0 \exp[\pm j\omega_V t] \tag{19}$$

Now,
$$p(t) = \alpha(t)E(t) \tag{20}$$

Using Equations (18) and (19), $p(t)$ can be obtained as

$$p(t) = \alpha_0 E_0 \exp[j\omega_P t] + \left(\frac{\partial \alpha}{\partial x}\right)_{x_0} dx_0 E_0 \exp\left[j(\omega_P \pm \omega_V)t\right] \tag{21}$$

The polarization vector P is defined as dipole moment per unit volume. If there are N dipoles per unit volume then,

$$P(t) = N\alpha_0 E_0 \exp[j\omega_P t] + \left(\frac{\partial \alpha}{\partial x}\right)_{x_0} dx_0 N E_0 \exp\left[j(\omega_P \pm \omega_V)t\right] \tag{22}$$

This expression consists of two parts. The first part corresponds to linear optical phenomenon, and relative to incident radiation, it remains unshifted. The second part is nonlinear because the output frequency is different from input one.
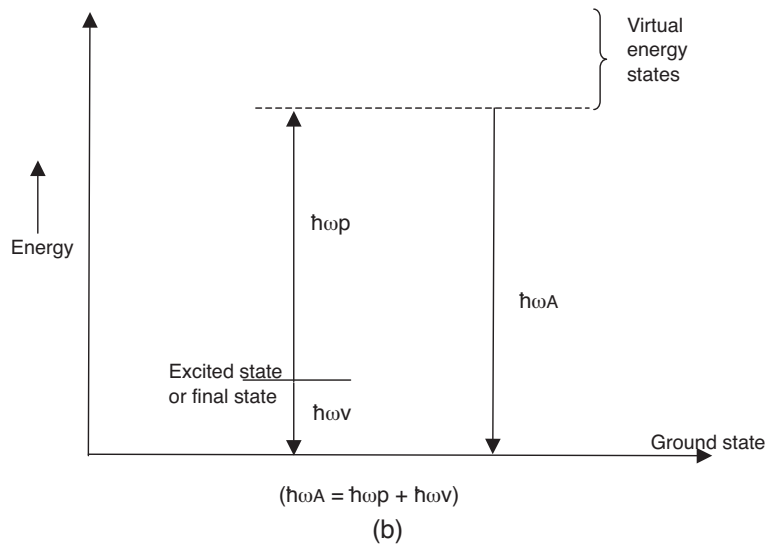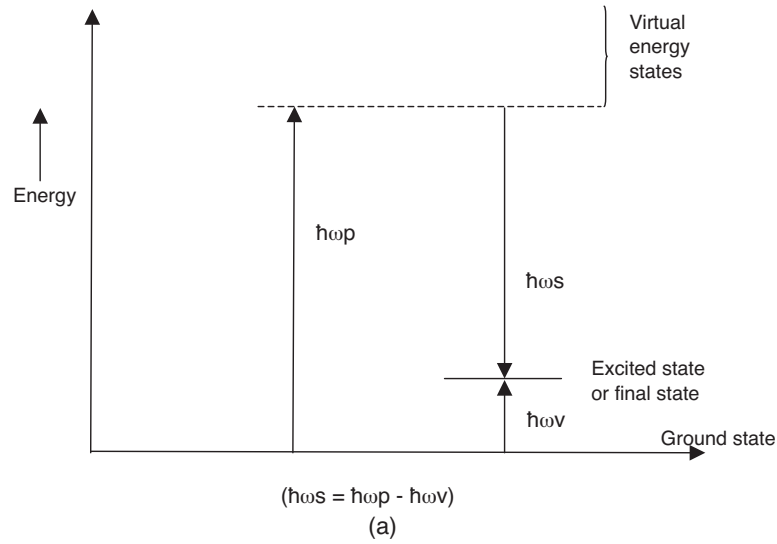

$(\hbar\omega s = \hbar\omega p - \hbar\omega v)$

(a)

$(\hbar\omega A = \hbar\omega p + \hbar\omega v)$

(b)

Figure 7. (a) Stokes scattering process. (b) Anti-Stokes scattering process.

The scattered light with lower energy ($\hbar\omega_S < \hbar\omega_P$) corresponds to Stokes scattering (Figure 7(a)) and with higher energy ($\hbar\omega_A > \hbar\omega_P$) one has anti-Stokes scattering phenomenon (Figure 7(b)). In thermal equilibrium situation, because of greater population of the ground state in comparison to vibrational state, the Stokes scattering dominates. At low illumination levels, the spontaneous Raman scattering occurs because in this situation molecules contributing to the process are vibrating independently and hence scattered light is non-directional. But when the intensity level becomes high the molecules may be considered as an array of vibrating oscillators and the generated photons aligned in phase or behave coherently.   This results in stimulated Raman scattering (SRS).

3.2. The Raman Process

In quantum mechanical picture, Raman effect is a process, which involves double quantum molecular transition. In most frequent Stokes scattering process, the energy of incident photon ($\hbar\omega_P$) is reduced to lower level ($\hbar\omega_S$) and difference energy is transferred to molecule of silica in form of kinetic energy, inducing stretching, bending or rocking of the molecular bonds [21].   The Raman shift $\omega_R (= \omega_P - \omega_S)$ is dictated by the vibrational energy levels of silica.

The Stokes Raman process is also known as the forward Raman process (Figure 7(a)) and the energy conservation for the process is

$$E_g + \hbar\omega_P = E_f + \hbar\omega_S$$

where E_g and E_f are ground state and final state energies respectively.

The absorption of incident photon, the emission of scattered photon and transition of the molecule to excited state occurs simultaneously in one step.   Therefore, Raman process may be considered as a single step process, which makes stimulated Raman effect possible whenever sufficient numbers of Stokes photons are created.   At this juncture it is worth to mention that, in step wise transitions, the absorption and emission of photons occur through two consecutive single quantum transitions via a third molecular energy level. Such transitions are associated with complete disruption of the phase of a molecule after each act of absorption and emission of a single quantum.

The Figure 8 explains composite stimulated Raman scattering. The nonlinear polarization causes an electron to be excited to an upper virtual state.   The energy and hence frequency of optical phonon is dictated by the material concerned so, it may be predetermined. The selection of different pump frequencies results in stimulated emission at
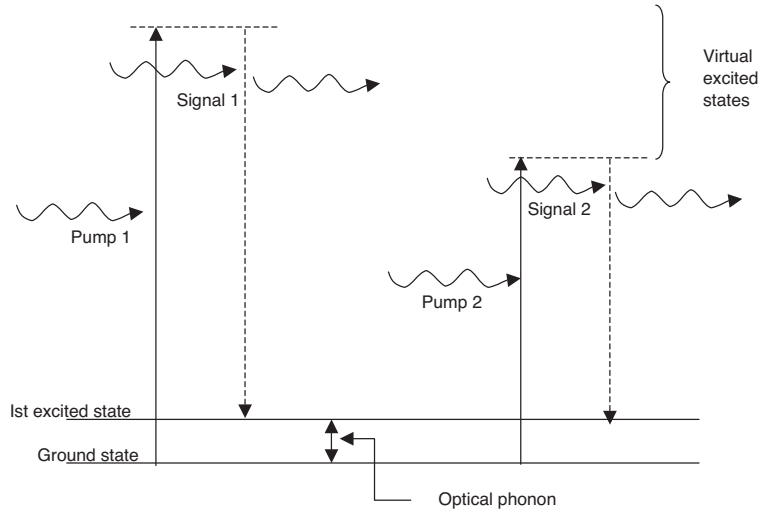
Figure 8. Stimulated Raman scattering for two pump wavelengths.

many frequencies. It is this feature, which is exploited for amplification in WDM systems through Raman amplifier [22].

The stimulated scattering can transfer photons from signal to pump wave as well as from pump to signal wave. There is net transfer of photons from pump to signal (gain coefficient is positive and signal is amplified) in case of Stokes scattering, while in case of anti-Stokes scattering net transfer of photons from signal to pump occurs. In this case gain coefficient is negative and there is attenuation (Inverse Raman Effect) in signal strength. Sometimes growth in anti-Stokes scattering is also observed but it is actually due to four-wave mixing phenomenon. It is this growth, which is responsible for a powerful spectroscopic technique known as coherent anti-Stokes Raman scattering (CARS).

Both Stokes and anti-Stokes scattering are temperature depen-dent [23] processes with following properties.

1. The anti-Stokes scattering is weaker than the Stokes scattering process.

2. The Stokes and anti-Stokes scattering strength increases with temperature.

3. The strength of Stokes scattering rises to a constant value and the strength of anti-Stokes scattering decays to zero at low temperature.

4. The anti-Stokes scattering strength approaches to Stokes scattering strength at high temperatures.

5. The Stokes scattering may occur at zero Kelvin but anti-Stokes scattering does not happen at zero Kelvin.

3.3. SRS Spectrum

With classical electromagnetic concepts, the growth of stimulated Raman scattered signal intensity [1] is proportional to the product of the pump (I_P) and signal (I_S) intensities such that

$$\frac{dI_S}{dz} = g_R I_P I_S \tag{23}$$

here g_R is known as Raman-gain coefficient.

In order to generate stimulated emission, Stokes and pump waves must overlap spatially and temporally. The Raman-gain coefficient g_R is related to cross-section of spontaneous Raman scattering. The probability of a Raman scattering is proportional to the number of photons in pump wave per cross-sectional area and Raman cross-section. The material properties determine almost entirely the frequency spectrum of Raman cross-section because the Raman process is related to vibrational modes of the molecules of material. In crystalline materials, the Raman scattered light has a narrow bandwidth. The silica, which is main constituent of optical fiber, is amorphous in nature. The vibrational energy levels of such materials are not sharp but merge together and form a band [24]. In such a situation the Stokes frequency (ω_S) may differ from pump frequency (ω_P) over a wide range. Two major peaks occur at 13 THz and 15 THz for Raman shift $\omega_R = \omega_P - \omega_S$. For this shift, some miner peaks are also present in spectrum [25]. Therefore, the amorphous nature of silica is responsible for large bandwidth and multipeak nature of spectrum (Figure 9). This extension of Raman-gain over broad range in silica fiber [26] is exploited in broadband Raman amplifiers.

3.4. Threshold Power

The initial growth in stokes wave is given by Equation (23). Considering the fiber losses, the net growth in Stokes wave is written as

$$\frac{dI_S}{dz} = g_R I_P I_S - \alpha_S I_S \tag{24}$$

where α_S is attenuation coefficient.

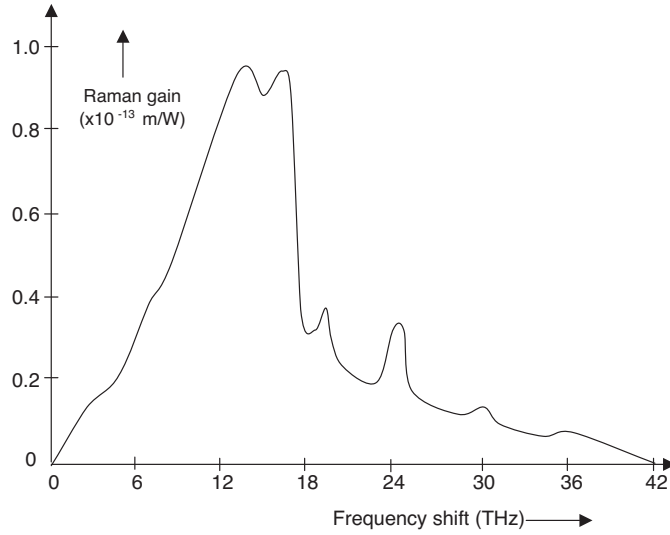**Figure 9.** Spectrum of Raman gain for silica at pump wavelength $1\,\mu$m.

For pump wave the coupled equation can be written as

$$\frac{dI_P}{dz} = -\frac{\omega_P}{\omega_S} g_R I_P I_S - \alpha_P I_P \tag{25}$$

Equations (24) and (25) are known as coupled wave equations for forward Raman scattering process [6]. In case of backward SRS process, Equation (25) remains same but in Equation (24) a minus sign must be added to dI_S/dz. This set of equation is similar to SBS process. The coupled equations for forward and backward SRS process may be understood phenomenologically by keeping in mind the processes through which photons appear in or disappear from each beam. In absence of losses due to fiber, Equations (24) and (25) can be reduced to

$$\frac{d}{dz}\left(\frac{I_S}{\omega_S} + \frac{I_P}{\omega_P}\right) = 0 \tag{26}$$

This equation dictates the conservation law on total number of photons in pump and Stokes waves during the SRS process.

The stimulatation occurs in Raman process when pump power exceeds a certain power level known as threshold power. In order to grow the stimulated scattering, the stimulated gain must exceed linear loss. In fact this is the origin of threshold power.

SRS can occur in both directions i.e., forward and backward direction in optical fibers. The beat frequency $(\omega_P - \omega_S)$ drives the molecular oscillations. These oscillations are responsible for increment in amplitude of scattered wave which in turn enhances the molecular oscillations. In this way a positive feedback loop is setup. It results in SRS process. The feedback process is governed by coupled Equations (24) and (25).

In case of forward SRS process the pump depletion can be neglected for estimating the Raman threshold [11]. Therefore first term on right hand side of Equation (25) can be neglected.

$$\frac{dI_P}{dz} = -\alpha_P I_P \qquad (27)$$

Solution of this equation can be written as

$$I_P(z) = I_0 \exp[-\alpha_P z] \qquad (28)$$

With Equation (24) and (28) we may have,

$$I_S(L) = I_S(0) \exp[g_R I_0 L_{eff} - \alpha_P L] \qquad (29)$$

where effective length, $L_{eff} = \frac{1 - \exp[-\alpha_P L]}{\alpha_P}$.

Practically, SRS builds up from spontaneous Raman scattering occurring throughout the fiber length. The Stokes power can be calculated by considering amplification of each frequency component of energy $\hbar\omega$ according to Equation (29) and integrating over the whole range of Raman-gain spectrum, i.e.,

$$P_S(L) = \int_{-\infty}^{\infty} \hbar\omega \exp\left[g_R(\omega_P - \omega)I_0 L_{eff} - \alpha_S L\right] d\omega \qquad (30)$$

The main contribution to the integral comes from narrow region around the gain peak. So using $\omega = \omega_S$, above equation can be written as

$$P_S(L) = \int_{-\infty}^{\infty} \hbar\omega_S \exp\left[g_R(\omega_P - \omega_S)I_0 L_{eff} - \alpha_S L\right] d\omega_S \qquad (31)$$

In terms of power, the Equation (28) may be written as under

$$P_P(L) = P_0 \exp[-\alpha_P L] \qquad (32)$$

where $P_0 = I_0 A_{eff}$ is input pump power and A_{eff} is effective core area. The Raman threshold is also defined as the input pump power at which

the Stokes power becomes equal to the pump power at the fiber output. So,

$$P_S(L) = P_P(L) = P_0 \exp[-\alpha_P L] \qquad (33)$$

With assumption $\alpha = \alpha_S$, the threshold condition may be approximated [11] by using Equation (31) and (33).

$$P_{th} \approx \frac{16 A_{eff}}{g_R L_{eff}} \qquad (34)$$

Exactly a similar analysis can be carried out for backward SRS, and threshold power can be approximated as

$$P_{th} \approx \frac{20 A_{eff}}{g_R L_{eff}} \qquad (35)$$

Clearly the threshold for forward SRS is reached first at a given pump power. The backward SRS is generally not observed in fibers.

The Equation (34) is derived by using many approximations, but it is able to predict the Raman threshold quite accurately. For a typical optical communication system at 1550 nm, $A_{eff} \approx 50\,\mu\text{m}^2$, $L_{eff} \approx 20$ km and $g_R \approx 6 \times 10^{-14}$ m/W. With these values Equation (34) predicts $P_{th} \approx 570$ mW. As channel powers in optical communication systems are typically below 10 mW, SRS process is not a limiting factor for single-channel lightwave systems. However it affects the performance of WDM systems considerably.

3.5. Reduction in SRS Penalty

Many schemes can be applied for reduction of power penalty in SRS process [14, 15], such as,

1. Presence of dispersion reduces the SRS penalty. In presence of dispersion, signals in different channels travel at different velocities and hence reducing chances of overlap between pulses propagating at different wavelengths.

2. By decreasing channel spacing SRS penalty can be reduced.

3. The power level should be kept below threshold level which requires the reduction in distance between amplifiers [27]. The SRS imposed limitations on the maximum transmit power per channel is shown in Figure 10.
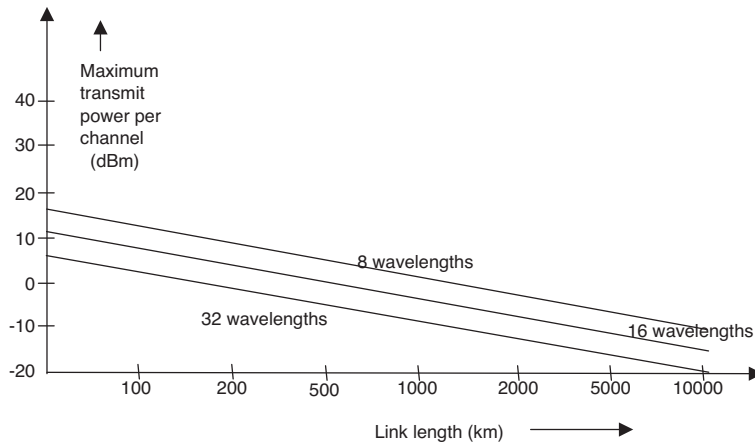
Figure 10. SRS produced limitation on maximum transmit power per channel. Channel spacing $= 0.8$ nm, and amplifiers are spaced 80 km apart.

3.6. Applications of SRS Phenomenon

The SRS process is exploited in many applications, which includes,

Raman Fiber Laser

Fiber based Raman lasers [28, 29] are developed by employing the SRS phenomenon. The Figure 11 shows a schematic of Raman laser. The partially reflecting mirrors M_1 and M_2 form a Febry-Perot cavity. Inside the cavity a piece of single mode fiber is placed in which SRS process occurs due wavelength-selective feedback for the Stokes light. This results in intense output. The spatial dispersion of various Stokes wavelengths allows tuning of the laser wavelength through an intra-cavity prism. The Raman amplification during a round trip should be as large as to compensate the cavity losses, and this determines the Raman threshold power.
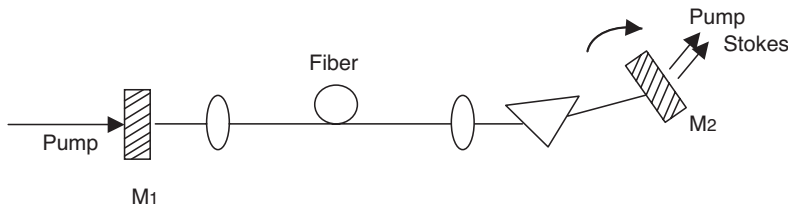

Figure 11. Schematic representation of a tunable Raman laser.

Higher-order Stokes wavelengths are generated inside the fiber at high pump powers. Again these wavelengths are dispersed spatially by the intra-cavity prism in association with separate mirrors for each Stokes beam. Such kind of Raman laser can be operated at several wavelengths simultaneously.

Raman Fiber Amplifier

The SRS phenomenon may be applied to provide optical amplification within optical fibers. The SRS process in fiber causes energy transfer from the pump to the signal. The Raman amplification may occur at any wavelength as long as appropriate pump laser is available. There are three basic components of Raman amplifier: pump laser, wavelength selective coupler and fiber gain medium. A schematic diagram is shown in Figure 12. Raman amplification exhibits advantages of self phase matching and broad gain-bandwidth which is advantageous in wavelength division multiplexed systems [30].
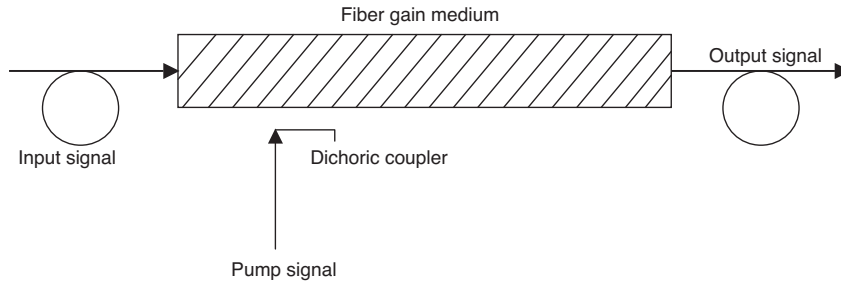
Figure 12. Schematic of Raman fiber amplifier.

Raman amplification may be realized as a continuous amplification along the fiber which let the signal never to become too low. Raman amplifier is bidirectional in nature and more stable.

Eye-Safe Laser

Fundamentally eye-safe laser utilizes stimulated Raman scattering phenomenon. Using a special s-polarized reflective resonator, a beam of an eye-safe laser with 31.8 mJ output energy and 2.0 ns pulse width can be obtained [40]. In such resonator configuration the length of the Raman resonator is shorter than the fundamental radiation resonator. Such eye-safe laser has the highest output energy and shortest pulse width among the Nd:KGW lasers.

4. COMPARISON OF RAMAN AND BRILLOUIN PROCESSES

Inspite of many similarities between SBS and SRS, the SBS differs from SRS in several ways.

1. The Brillouin scattering occurs due to Bragg type scattering from propagating acoustic wave, i.e., bulk motion of large number of molecules are involved. The Raman scattering is result of individual molecular motion.
2. The SBS occurs only in backward direction whereas SRS can occur in both directions, i.e., forward and backward.
3. Brillouin shift originates from the photon-acoustic phonon interaction while Raman shift is due to photon-optical phonon interaction. The SBS Stokes shift is smaller by three orders of magnitudes as compared to SRS Stokes shift.
4. The Brillouin gain bandwidth is extremely narrow in comparison of Raman gain bandwidth.
5. The threshold power level for SBS is quit low to that of SRS.
6. The Raman scattering process is isotropic and occurs in all directions whereas it is not so in case of Brillouin scattering.
7. The strength of Raman scattering is independent of the disorder of the material, but Brillouin scattering depends on the disorder of the material.

5. COMPARISON OF KERR AND SCATTERING EFFECTS

Kerr and scattering nonlinear effects are compared as under.

1. Kerr-nonlinear effects are due intensity dependence of refractive index, whereas this does not happen in case of nonlinear scattering effects.
2. Kerr-nonlinearities are elastic in the sense that they involve no energy transference. Nonlinear scattering effects are inelastic, i.e., energy transfer occurs from pump wave to Stokes wave.
3. No population inversion is needed in case of Kerr-nonlinear effects, while it is needed for nonlinear scattering effects (SRS and SBS).
4. Characteristics of the medium determine the features of the scattering effects, but in general, such is not case for Kerr-nonlinear effects.

6. CONCLUSION

Stimulated Brillouin and stimulated Raman scattering phenomenon is discussed. Normally both phenomenon put limitation on optical systems. But with suitable system arrangement they can be exploited in many applications. Typical threshold power for SBS is about 1.3 mW while for SRS, it is about 570 mW. The typical value of channel power in optical systems is below 10 mW. Therefore, SRS is not a limiting factor for single-channel lightwave systems while SBS puts limitations on such systems.

ACKNOWLEDGMENT

REFERENCES

1. Boyd, R. W., *Nonlinear Optics*, Academic Press, SanDiego, CA, 1992.

2. Shen, Y. R. and N. Bloembergen, "Theory of stimulated brillouin and raman scattering," *Phys. Rev. A*, Vol. 137, 1787–1805, 1965.

3. Singh, S. P. and N. Singh, "Nonlinear effects in optical fibers: origin, management and applications," *Progress In Electromagnetics Research*, PIER 73, 249–275, 2007.

4. Buckland, E. L. and R. W. Boyd, "Electrostrictive contribution to the intensity-dependent refractive index of optical fiber," *Opt. Lett.*, Vol. 21, 1117–1119, 1996.

5. Buckland, E. L. and R. W. Boyd, "Measurement of the frequency response of the electrostrictive nonlinearity in optical fiber," *Opt. Lett.*, Vol. 22, 676–678, 1997.

6. Agrawal, G. P., *Nonlinear Fiber Optics*, 3rd edition, Academic Press, SanDiego, CA, 2001.

7. Nikles, M., L. Thevenaz, and P. A. Robert, "Brillouin gain spectrum characterization in single-mode optical fiber," *J. Lightwave. Tech.*, Vol. 15, 1842–1851, 1997.

8. Sternklar, S. and E. Granot, "Narrow spectral response of a Brillouin amplifier," *Opt. Lett.*, Vol. 28, 977–979, 2003.

9. Cotter, D., "Observation of stimulated Brillouin scattering in low-loss silica fiber at 1.3 µm," *Electron. Lett.*, Vol. 18, 495–496, 1982.

10. Tkach, R. W., A. R. Chraplyvy, and R. M. Derosier, "Spontaneous

Brillouin scattering for single-mode optical fiber characterization," *Electron. Lett.*, Vol. 22, 1011–1013, 1986.

11. Smith, R. G., "Optical power handling capacity of low optical fibers as determined by stimulated Raman and Brillouin scattering," *Appl. Opt.*, Vol. 11, 2489–2494, 1972.

12. Stolen, R. J., "Polarization effects in Raman and Brillouin lasers," *IEEE J. Quantum Electron.*, Vol. QE-15, 1157–1160, 1979.

13. Mao, X. P., R. W. Tkach, A. R. Chraplyvy, R. M. Jopson, and R. M. Dorosier, "Stimulated Brillouin threshold dependence on fiber type and uniformity," *IEEE Photonics Tech. Lett.*, Vol. 4, 66–69, 1992.

14. Ramaswami, R. and K. Sivarajan, *Optical Networks—A Practical Perspective*, Morgan Kaufmann Pub. Inc., San Francisco, 1998.

15. Forghieri, F., R. W. Tkach, and A. R. Chraplyvy, "Fiber nonlinerities and their impact on transmission systems," *Optical Fiber Telecommunications-III*, I. P. Kaminow and T. L. Koch (eds.), Vol. A, Academic Press, New York, 1997.

16. Fishman, D. A. and J. A. Nagel, "Degradation due to stimulated Brillouin scattering in multigigabit intensity-modulated fiber-optic systems," *J. Lightwave Tech.*, Vol. 11, 1721–1728, 1993.

17. Kee, H. H., G. P. Lees, and T. P. Newson, "All-fiber system for simultaneous interrogation of distributed strain and temperature sensing by spontaneous Brillouin scattering," *Opt. Lett.*, Vol. 25, 1–3, 2000.

18. Kotate, K. and M. Tanaka, "Distributed fiber Brillouin strain sensing with 1-cm spatial resolution by correlation-based continuous-wave technique," *IEEE Photon. Tech. Lett.*, Vol. 14, 179–181, 2002.

19. Pannell, C. N., P. St. J. Russell, and T. P. Newson, "Stimulated Brillouin scattering in optical fibers: the effect of optical amplification," *J. Opt. Soc. Amer. B*, Vol. 10, 684–690, 1993.

20. Lan, G.-L., P. K. Banerjee, and S. S. Mitra, "Raman scattering in optical fibers," *J. of Raman Spectrosc.*, Vol. 11, 416–423, 1981.

21. Shibate, N., M. Horigudhi, and T. Edahiro, "Raman spectra of binary high-silica glasses and fibers containing GeO_2, P_2O_5 and B_2O_3," *J. of Non-crystalline Solids*, Vol. 45, 115–126, 1981.

22. Bromage, J., "Raman amplification for fiber communication systems," *J. Lightwave. Tech.*, Vol. 22, 79–93, 2004.

23. Lewis, S. A. E., S. V. Chernikov, and J. R. Taylor, "Temperature dependent gain and noise in fiber Raman amplifier," *Opt. Lett.*, Vol. 24, 1823–1825, 1999.

24. Stolen, R. H., E. P. Ippen, and A. R. Tynes, "Raman oscillation in glass optical waveguide," *Appl. Phys. Lett.*, Vol. 20, 62–64, 1972.

25. Stolen, R. H. and E. P. Ippen, "Raman gain in glass optical waveguides," *Appl. Phys. Lett.*, Vol. 22, 276–278, 1973.

26. Tomlinson, W. J. and R. H. Stolen, "Nonlinear phenomenon in optical fibers," *IEEE Commun. Mag.*, Vol. 26, No. 4, 36–44, 1988.

27. Ohmori, Y., Y. Sasaki, and T. Edahiro, "Fiber-length dependence of critical power for stimulated Raman scattering," *Electron. Lett.*, Vol. 17, No. 17, 593–594, 1981.

28. Back, S. H. and W. B. Roh, "Single-mode Raman fiber laser based on a multimode fiber," *Opt. Lett.*, Vol. 29, 153–155, 2004.

29. Karpov, V. I., E. M. Dianov, V. M. Paramonoc, O. I. Medvedkov, M. M. Bubnov, S. L. Semyonov, S. A. Vasiliev, V. N. Protopopov, D. N. Egorova, V. F. Hopkin, A. N. Guryanov, M. P. Bachymki, and W. Clements, "Laser-diode pumped phosphosilicate-fiber Raman laser with an output power of 1 W at 1.48 nm," *Opt. Lett.*, Vol. 24, 887–889, 1999.

30. Aoki, Y., "Properties of Raman amplifier and their applicability to digital optical communication systems," *J. Lightwave. Tech.*, Vol. LT-6, 1225–1239, 1988.

31. Bars, F. and L. Resnic, "On the theory of the electromagnetic wave-propagation through inhomogeneous dispersive media," *Journal of Electromagnetic Waves and Applications*, Vol. 19, No. 7, 925–931, 2005.

32. Wang, S., X. Guan, D. Wang, X. Ma, and Y. Su, "Electromagnetic scattering by mixed conducting/dielectric objects using high-order MOM," *Progress In Electromagnetics Research*, PIER 66, 51–63, 2006.

33. Anupam, R., M. Chandran, C. K. Anandan, P. Mohanan, and K. Vasudevan, "Scattering behavior of fractal based metallo-dielectric structures," *Progress In Electromagnetics Research*, PIER 69, 323–339, 2007.

34. Brown, A. W., B. G. Colpitts, and K. Brown, "Dark-pulse Brillouin optical time-domain sensor with 20-mm spatial resolution," *J. of Lightwave Technology*, Vol. 25, No. 1, 381–386, 2007.

35. Misas, C. J., P. Petropoulos, and D. J. Richardson, "Slowing of pulses to c/10 with subwatt power levels and low latency using Brillouin amplification in a bismuth-oxide optical fiber," *J. of Lightwave Technology*, Vol. 25, No. 1, 216–221, 2007.

36. Brown, K. C., T. H. Russell, T. G. Alley, and W. B. Roh, "Passive combination of multiple beams in an optical fiber via stimulated Brillouin scattering," *Optics Letters*, Vol. 32, No. 9, 1047–1049, 2007.

37. Song, K. Y., M. Herraez, and L. Thevenaz, "Observation of pulse delaying and advancement in optical fibers using stimulated Brillouin scattering," *Optics Express*, Vol. 13, No. 1, 82–88, 2005.

38. Kalosha, V. P., L. Chen, and X. Bao, "Slow and fast light via SBS in optical fibers for short pulses and broadband pump," *Optics Express*, Vol. 14, No. 26, 12693–12703, 2006.

39. Zou, L., X. Bao, F. Ravet, and L. Chen, "Distributed Brillouin fiber sensor for detecting pipeline buckling in an energy pipe under internal pressure," *Applied Optics*, Vol. 45, No. 14, 3372–3377, 2006.

40. Huang, J., J. Lin, R. Su, J. Li, H. Zheng, C. Xu, F. Shi, Z. Lin, J. Zhuang, W. Zeng, and W. Lin, "Short pulse eye-safe laser with a stimulated Raman scattering self-conversion based on a Nd:KGW crystal," *Optics Letters*, Vol. 32, No. 9, 1096–1098, 2007.